Synergy of semiconductor physics and electron pairing: route towards novel topological materials

Tadeusz DOMAŃSKI

M. Curie-Skłodowska University (Lublin)

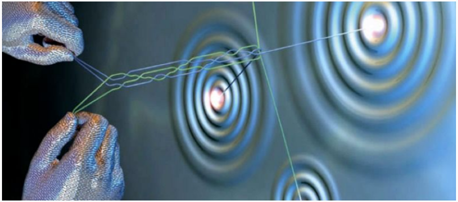

13-th Int. Conf. on "Ion implantation ..." **Kazimierz Dolny, 27 June 2022**

Electrons in solids

(primer)

Itinerant electrons in a lattice of periodically distributed ions

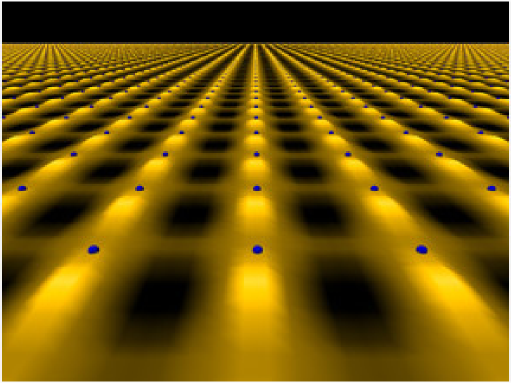

Itinerant electrons in a lattice of periodically distributed ions

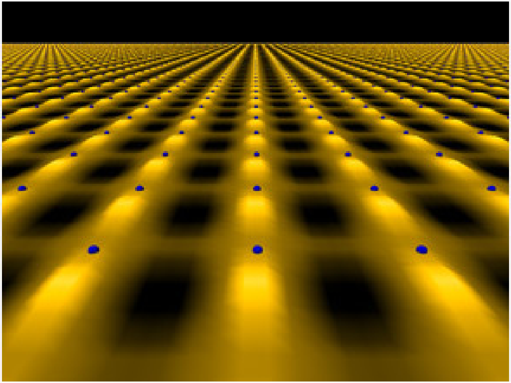

are described by the Bloch waves

$$\psi_{n,\vec{k}}(\vec{r}) = u_{n,\vec{k}}(\vec{r})\; e^{i\vec{k}\cdot\vec{r}}$$

Itinerant electrons in a lattice of periodically distributed ions

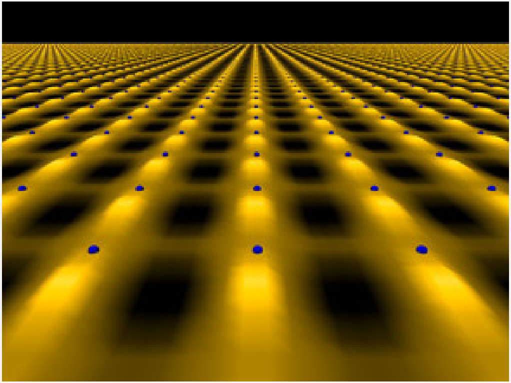

are described by the Bloch waves

$$\psi_{n,\vec{k}}(\vec{r}) = u_{n,\vec{k}}(\vec{r})\ e^{i\vec{k}\cdot\vec{r}}$$

where $u_{n,\vec{k}}(\vec{r}+\vec{R}) = u_{n,\vec{k}}(\vec{r})$ are translationally invariant.

These Bloch waves substituted to the Schrödinger equation

$$\hat{H}\,\psi_{n,\vec{k}}(\vec{r}) = \varepsilon_n(\vec{k})\psi_{n,\vec{k}}(\vec{r})$$

ELECTRONIC BAND-STRUCTURE

These Bloch waves substituted to the Schrödinger equation

$$\hat{H}\,\psi_{n,\vec{k}}(\vec{r}) = \varepsilon_n(\vec{k})\psi_{n,\vec{k}}(\vec{r})$$

imply eigen-energies $\varepsilon_n(\vec{k})$ forming the band-structure.

ELECTRONIC BAND-STRUCTURE

These Bloch waves substituted to the Schrödinger equation

$$\hat{H}\,\psi_{n,\vec{k}}(\vec{r}) = \varepsilon_n(\vec{k})\psi_{n,\vec{k}}(\vec{r})$$

imply eigen-energies $\varepsilon_n(\vec{k})$ forming the band-structure.

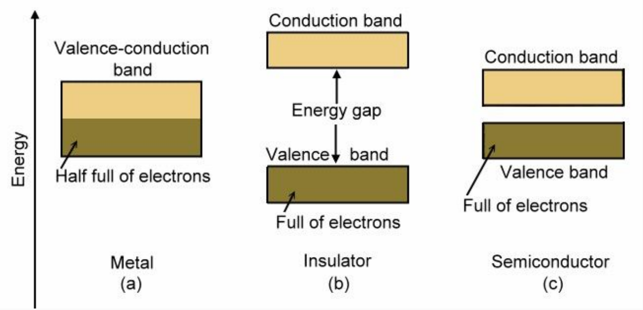

DOPING MECHANISM

The periodic lattice can be disrupted by introducing impurities:

DOPING MECHANISM

The periodic lattice can be disrupted by introducing impurities:

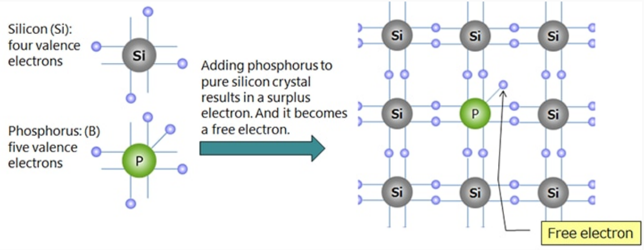

DOPING MECHANISM

The periodic lattice can be disrupted by introducing impurities:

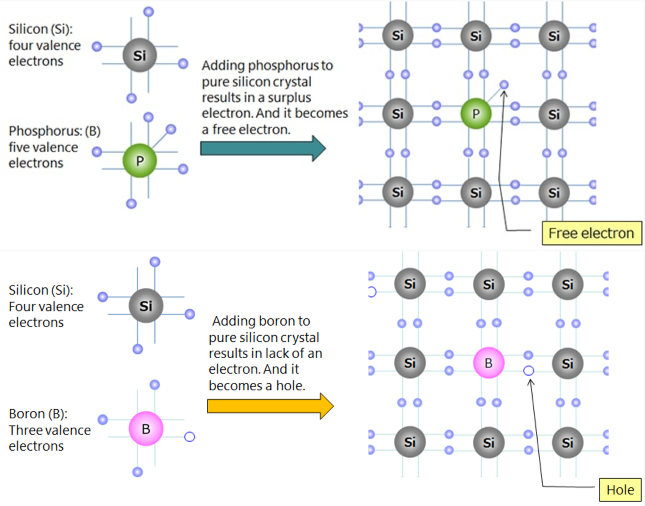

IN-GAP STATES INDUCED BY DOPING

Donors/acceptors contribute in-gap levels to electronic structure

Donors/acceptors contribute in-gap levels to electronic structure

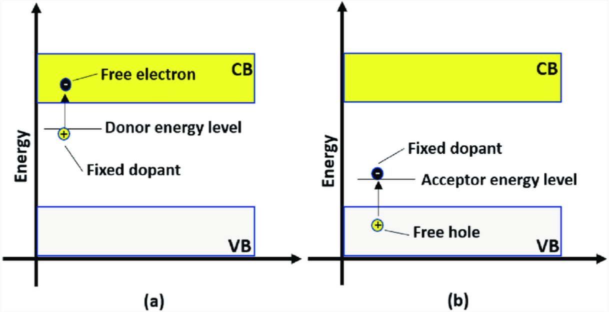

IN-GAP STATES INDUCED BY DOPING

Donors/acceptors contribute in-gap levels to electronic structure

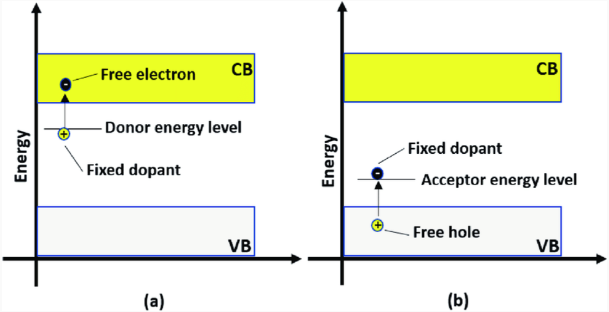

which provide charge carriers to the conductance/valence bands. This mechanism gave rise to modern technology.

IN-GAP STATES DUE TO BOUNDARIES

Different means to obtain the in-gap states (of insulators) have been recently considered due to topological reasons.

IN-GAP STATES DUE TO BOUNDARIES

Different means to obtain the in-gap states (of insulators) have been recently considered due to topological reasons.

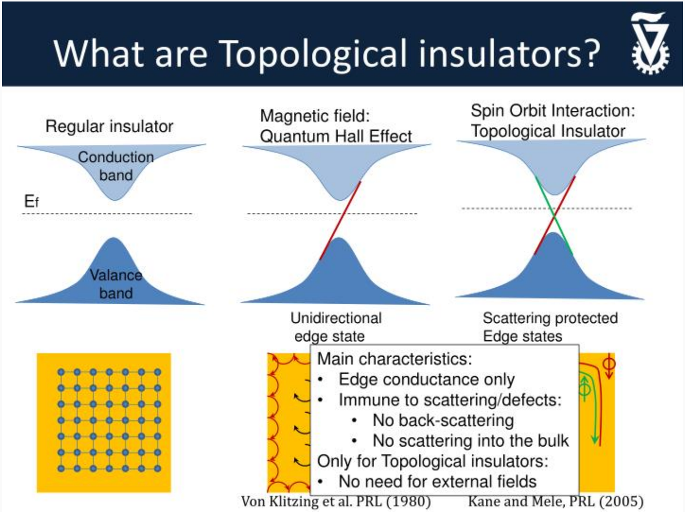

Comment on topology and its role in physics

EXAMPLE: CLASSICAL ELECTROSTATICS

The electric flux emanating from or flowing into a closed surface depends solely on the total charge enclosed inside it. Any shape of such surface and spatial charge distribution are irrelevant.

$$\oint \vec{E} \cdot \vec{dA} = \frac{Q}{\varepsilon_0}$$

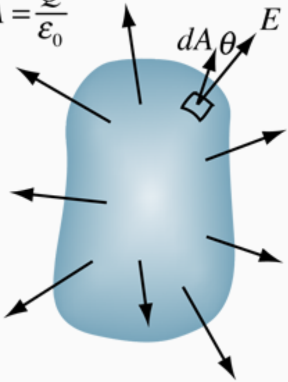

EXAMPLE: CLASSICAL ELECTROSTATICS

The electric flux emanating from or flowing into a closed surface depends solely on the total charge enclosed inside it. Any shape of such surface and spatial charge distribution are irrelevant.

$$\oint \vec{E} \cdot \vec{dA} = \frac{Q}{\varepsilon_0}$$

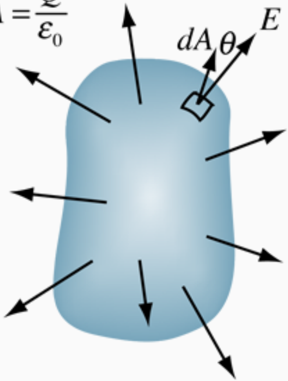

Johann Carl Friedrich Gauss (1777-1855)

CONCEPTS OF BERRY-OLOGY

Inspecting $\psi_{n,\vec{k}}(\vec{r}) = u_{n,\vec{k}}(\vec{r})\ e^{i\vec{k}\cdot\vec{r}}$ we can define the Berry connection

$$\vec{A}_n(\vec{k}) = \left\langle u_{n,\vec{k}}(\vec{r}) \middle| \, i\nabla_{\vec{k}} \, \middle| u_{n,\vec{k}}(\vec{r}) \right\rangle$$

CONCEPTS OF BERRY-OLOGY

Inspecting $\psi_{n,\vec{k}}(\vec{r}) = u_{n,\vec{k}}(\vec{r})\ e^{i\vec{k}\cdot\vec{r}}$ we can define the Berry connection

$$\vec{A}_n(\vec{k}) = \left\langle u_{n,\vec{k}}(\vec{r}) \right| i\nabla_{\vec{k}} \left| u_{n,\vec{k}}(\vec{r}) \right\rangle$$

which brings information on topological effects.

CONCEPTS OF BERRY-OLOGY

Inspecting $\psi_{n,\vec{k}}(\vec{r}) = u_{n,\vec{k}}(\vec{r})\ e^{i\vec{k}\cdot\vec{r}}$ we can define the Berry connection

$$\vec{A}_n(\vec{k}) = \left\langle u_{n,\vec{k}}(\vec{r}) \middle| i\nabla_{\vec{k}} \middle| u_{n,\vec{k}}(\vec{r}) \right\rangle$$

which brings information on topological effects. The Berry curvature

$$\vec{F}_n(\vec{k}) = \nabla_{\vec{k}} \times \vec{A}_n(\vec{k})$$

CONCEPTS OF BERRY-OLOGY

Inspecting $\psi_{n,\vec{k}}(\vec{r}) = u_{n,\vec{k}}(\vec{r})\ e^{i\vec{k}\cdot\vec{r}}$ we can define the Berry connection

$$\vec{A}_n(\vec{k}) = \left\langle u_{n,\vec{k}}(\vec{r}) \middle| i\nabla_{\vec{k}} \middle| u_{n,\vec{k}}(\vec{r}) \right\rangle$$

which brings information on topological effects. The Berry curvature

$$\vec{F}_n(\vec{k}) = \nabla_{\vec{k}} \times \vec{A}_n(\vec{k})$$

integrated along a closed path

$$\oint_C d\vec{k} \cdot \vec{F}_n(\vec{k})$$

CONCEPTS OF BERRY-OLOGY

Inspecting $\psi_{n,\vec{k}}(\vec{r}) = u_{n,\vec{k}}(\vec{r})\ e^{i\vec{k}\cdot\vec{r}}$ we can define the Berry connection

$$\vec{A}_n(\vec{k}) = \left\langle u_{n,\vec{k}}(\vec{r}) \middle| \, i\nabla_{\vec{k}} \, \middle| u_{n,\vec{k}}(\vec{r}) \right\rangle$$

which brings information on topological effects. The Berry curvature

$$\vec{F}_n(\vec{k}) = \nabla_{\vec{k}} \times \vec{A}_n(\vec{k})$$

integrated along a closed path

$$\oint_C d\vec{k} \cdot \vec{F}_n(\vec{k})$$

yields the Berry phase (often identical with the Chern number).

CONCEPTS OF BERRY-OLOGY

Inspecting $\psi_{n,\vec{k}}(\vec{r}) = u_{n,\vec{k}}(\vec{r})\ e^{i\vec{k}\cdot\vec{r}}$ we can define the Berry connection

$$\vec{A}_n(\vec{k}) = \left\langle u_{n,\vec{k}}(\vec{r}) \middle| i\nabla_{\vec{k}} \middle| u_{n,\vec{k}}(\vec{r}) \right\rangle$$

which brings information on topological effects. The Berry curvature

$$\vec{F}_n(\vec{k}) = \nabla_{\vec{k}} \times \vec{A}_n(\vec{k})$$

integrated along a closed path

$$\oint_C d\vec{k} \cdot \vec{F}_n(\vec{k})$$

yields the Berry phase (often identical with the Chern number).

When certain symmetries are imposed and a suitable path C is considered, the Berry phase is quantized and can be regarded as topological invariant which plays equivalent role to electric charge in the classical Gauss law.

TOPOLOGICAL PROPERTIES

- **Materials can be classified into 10 different categories according to: a) time-reversal, b) particle-hole and c) chiral symmetries.**

TOPOLOGICAL PROPERTIES

- **Materials can be classified into 10 different categories according to: a) time-reversal, b) particle-hole and c) chiral symmetries.**
- **Two samples belong to the same topological category, if there exists a continuous process connecting them (preserving the gap).**

TOPOLOGICAL PROPERTIES

- **Materials can be classified into 10 different categories according to: a) time-reversal, b) particle-hole and c) chiral symmetries.**
- **Two samples belong to the same topological category, if there exists a continuous process connecting them (preserving the gap).**
- **Topological transition can occur by closing/reopening the gap.**

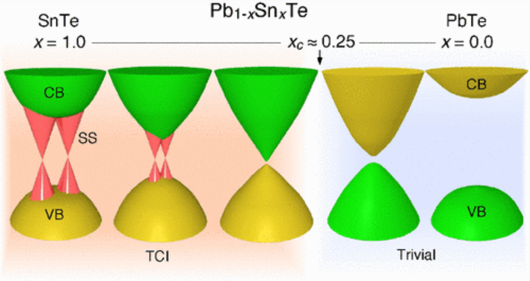

TOPOLOGICAL PROPERTIES

- Materials can be classified into 10 different categories according to: a) time-reversal, b) particle-hole and c) chiral symmetries.
- Two samples belong to the same topological category, if there exists a continuous process connecting them (preserving the gap).
- Topological transition can occur by closing/reopening the gap.

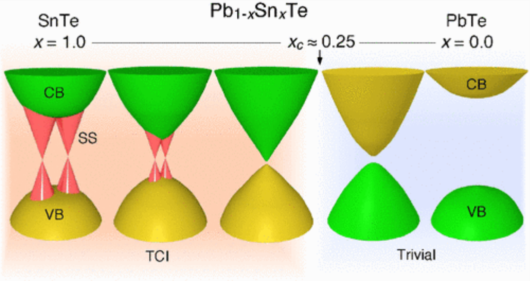

- Bulk-to-boundary correspondence assigns $2|\nu|$ edge modes related to the Chern number ν. These modes are topologically protected.

Similar concepts have been next adopted to superconductors, whose electronic spectrum is gaped due to the Cooper pairing

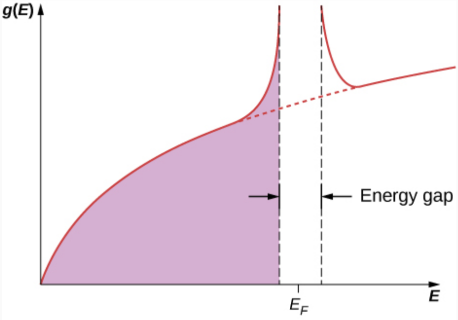

Similar concepts have been next adopted to superconductors, whose electronic spectrum is gaped due to the Cooper pairing

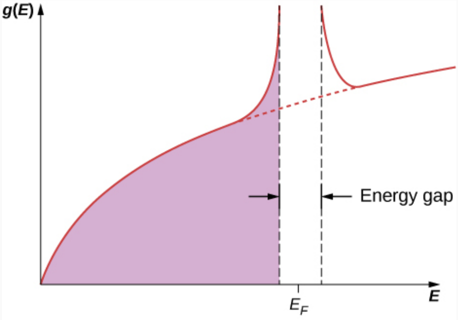

⇒ **Majorana quasiparticles**

TOPOLOGICAL SUPERCONDUCTORS

Similar concepts have been next adopted to superconductors, whose electronic spectrum is gaped due to the Cooper pairing

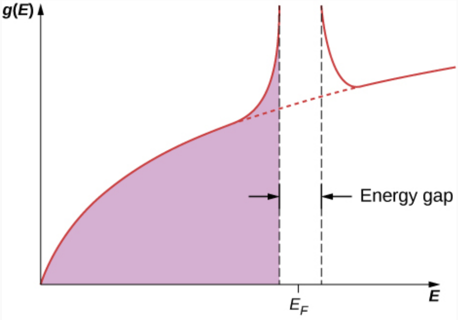

⇒ **Majorana quasiparticles**

⇒ **non-Abelian statistics**

Macroscopic superconductors

Perfect conductor

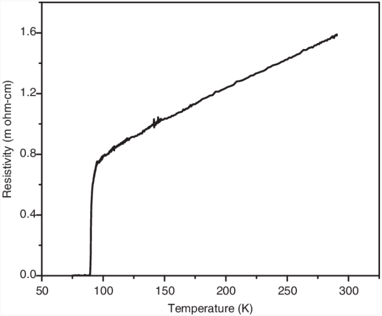

SUPERCONDUCTOR: PROPERTIES

Perfect conductor

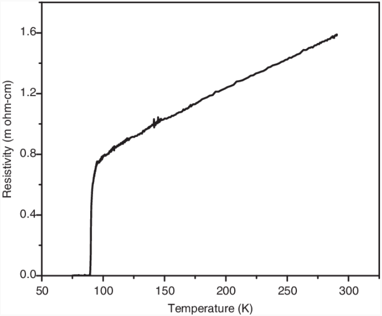

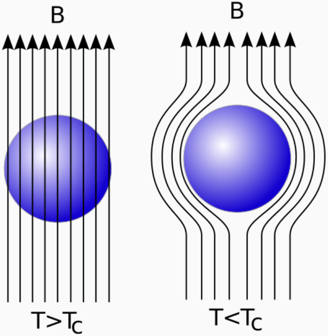

Perfect diamagnet

BCS (non-Fermi liquid) ground state :

$$|\mathbf{BCS}\rangle = \prod_k \left(u_k + v_k \, \hat{c}^\dagger_{k\uparrow} \, \hat{c}^\dagger_{-k\downarrow} \right) \, |\mathbf{vacuum}\rangle$$

BCS (non-Fermi liquid) ground state :

$$|\mathbf{BCS}\rangle = \prod_k \left(u_k + v_k \ \hat{c}^{\dagger}_{k\uparrow} \ \hat{c}^{\dagger}_{-k\downarrow} \right) \ |\mathbf{vacuum}\rangle$$

$|v_k|^2 \Rightarrow$ **probablity of occupied states** $(k\uparrow, -k\downarrow)$

ELECTRON PAIRING

BCS (non-Fermi liquid) ground state :

$$|\mathbf{BCS}\rangle = \prod_k \left(u_k + v_k \; \hat{c}^\dagger_{k\uparrow} \, \hat{c}^\dagger_{-k\downarrow} \right) \; |\mathbf{vacuum}\rangle$$

$|v_k|^2 \Rightarrow$ **probablity of occupied states** $(k\uparrow, -k\downarrow)$

$|u_k|^2 \Rightarrow$ **probablity of unoccupied states** $(k\uparrow, -k\downarrow)$

ELECTRON PAIRING

BCS (non-Fermi liquid) ground state :

$$|\mathbf{BCS}\rangle = \prod_k \left(u_k + v_k \; \hat{c}^\dagger_{k\uparrow} \; \hat{c}^\dagger_{-k\downarrow} \right) \; |\mathbf{vacuum}\rangle$$

$|v_k|^2 \Rightarrow$ **probablity of occupied states** $(k \uparrow, -k \downarrow)$

$|u_k|^2 \Rightarrow$ **probablity of unoccupied states** $(k \uparrow, -k \downarrow)$

Bogoliubov quasiparticle = superposition of a particle and hole

$$\begin{aligned} \hat{\gamma}_{k\uparrow} &= u_k \hat{c}_{k\uparrow} + v_k \hat{c}^\dagger_{-k\downarrow} \\ \hat{\gamma}^\dagger_{-k\downarrow} &= -v_k \hat{c}_{k\uparrow} + u_k \hat{c}^\dagger_{-k\downarrow} \end{aligned}$$

ELECTRON PAIRING

BCS (non-Fermi liquid) ground state :

$$|\mathrm{BCS}\rangle = \prod_k \left(u_k + v_k \, \hat{c}^\dagger_{k\uparrow} \, \hat{c}^\dagger_{-k\downarrow} \right) \; |\mathrm{vacuum}\rangle$$

$|v_k|^2 \Rightarrow$ **probablity of occupied states** $(k\uparrow, -k\downarrow)$

$|u_k|^2 \Rightarrow$ **probablity of unoccupied states** $(k\uparrow, -k\downarrow)$

Bogoliubov quasiparticle = superposition of a particle and hole

$$\begin{aligned} \hat{\gamma}_{k\uparrow} &= u_k \hat{c}_{k\uparrow} + v_k \hat{c}^\dagger_{-k\downarrow} \\ \hat{\gamma}^\dagger_{-k\downarrow} &= -v_k \hat{c}_{k\uparrow} + u_k \hat{c}^\dagger_{-k\downarrow} \end{aligned}$$

Charge is conserved modulo-2e due to Bose-Einstein condensation of the Cooper pairs.

Quasiparticle spectrum of conventional superconductors consists of two Bogoliubov (p/h) branches, gaped around E_F

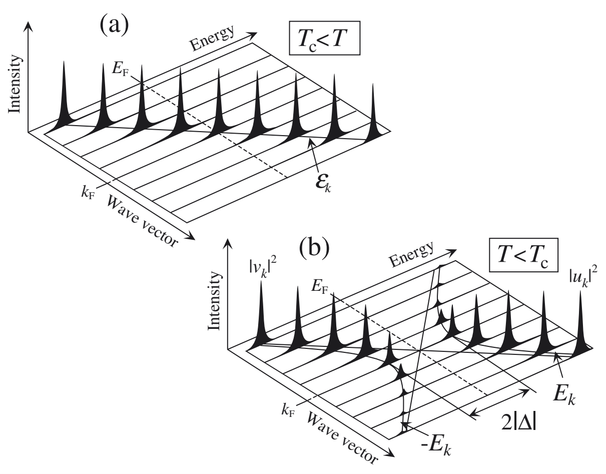

PARTICLE VS HOLE

In all superconductors the particle and hole degrees of freedom are mixed with one another

PARTICLE VS HOLE

In all superconductors the particle and hole degrees of freedom are mixed with one another (this is particularly evident near E_F)

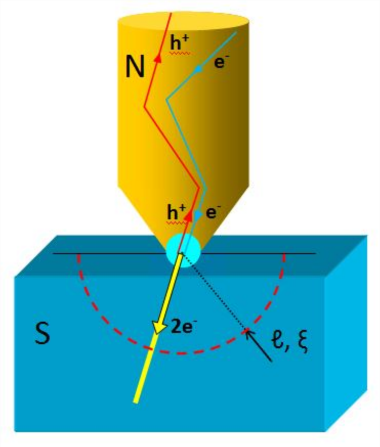

PARTICLE VS HOLE

Let us consider the interface of metal N and superconductor S

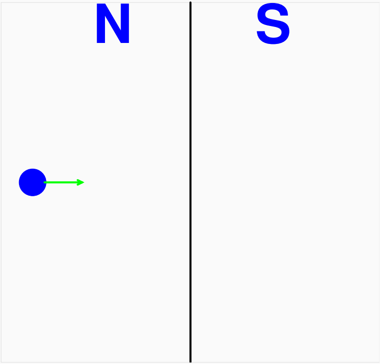

where incident electron ...

PARTICLE VS HOLE

Let us consider the interface of metal N and superconductor S

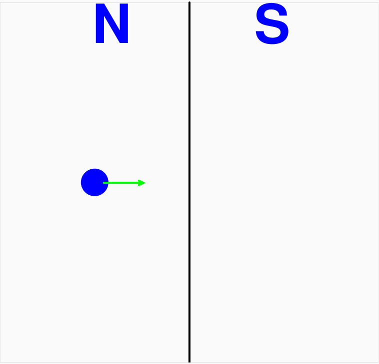

where incident electron ...

PARTICLE VS HOLE

Let us consider the interface of metal N and superconductor S

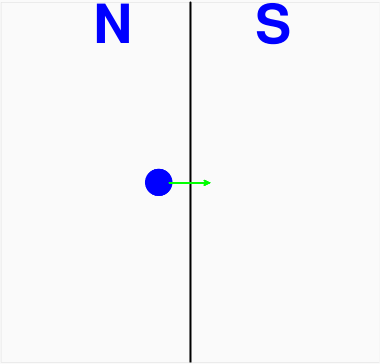

where incident electron ...

PARTICLE VS HOLE

Let us consider the interface of metal N and superconductor S

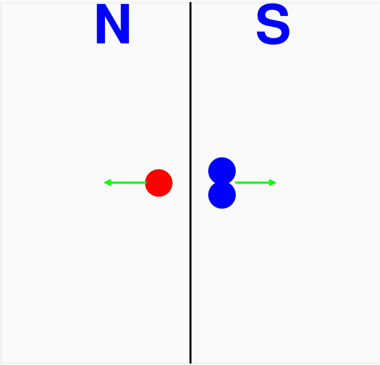

where incident electron is converted into: Cooper pair + hole.

PARTICLE VS HOLE

Let us consider the interface of metal N and superconductor S

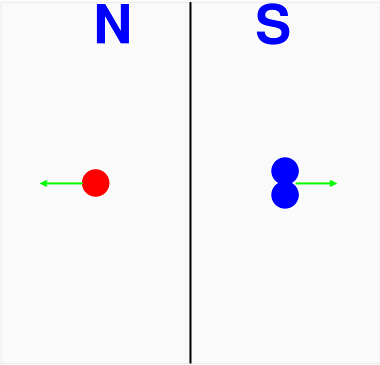

where incident electron is converted into: Cooper pair + hole.

PARTICLE VS HOLE

Let us consider the interface of metal N and superconductor S

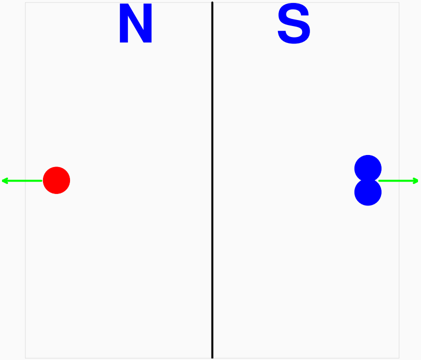

where incident electron is converted into: Cooper pair + hole.

Impurities in superconductors

IMPURITY IN BULK SUPERCONDUCTOR

Typical spectrum of a single impurity in s-wave superconductor:

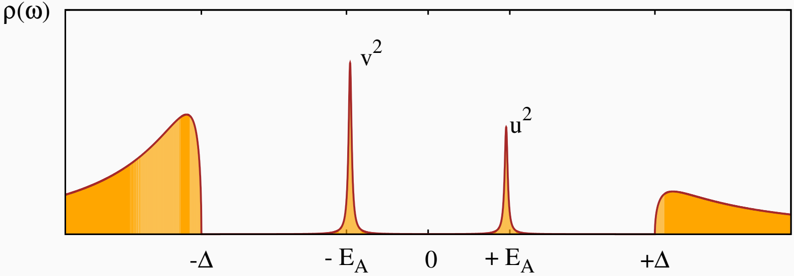

Bound states appearing in the subgap region $E \in \langle -\boldsymbol{\Delta}, \boldsymbol{\Delta} \rangle$

IMPURITY IN BULK SUPERCONDUCTOR

Typical spectrum of a single impurity in s-wave superconductor:

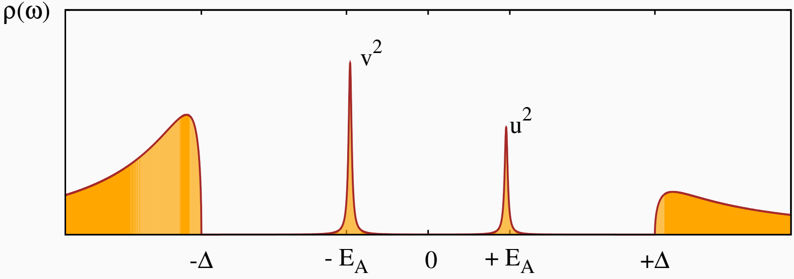

Bound states appearing in the subgap region $E \in \langle -\Delta, \Delta \rangle$

are dubbed Yu-Shiba-Rusinov (or Andreev) quasiparticles.

Magnetic chains

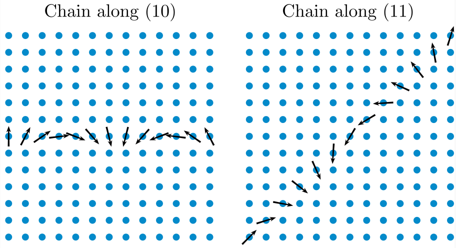

MAGNETIC OBJECTS IN SUPERCONDUCTORS

Magnetic chains

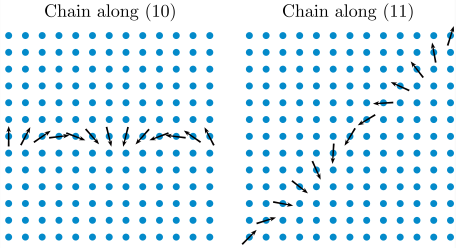

or magnetic islands

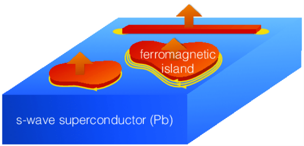

MAGNETIC OBJECTS IN SUPERCONDUCTORS

Magnetic chains

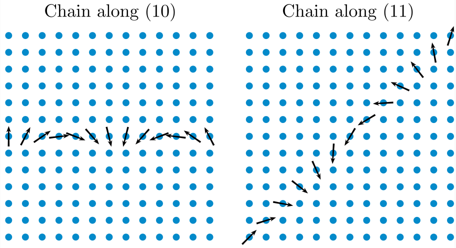

or magnetic islands

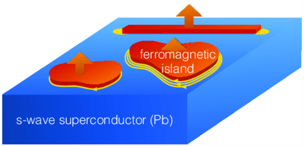

develop their in-gap bound states in a form of the Shiba-bands.

MAGNETIC OBJECTS IN SUPERCONDUCTORS

Magnetic chains

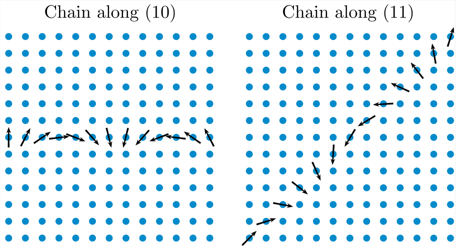

or magnetic islands

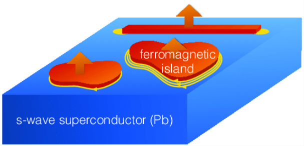

develop their in-gap bound states in a form of the Shiba-bands.

For specific magnetic textures of such chains and/or islands there appears topologically non-trivial superconducting state, hosting the Majorana boundary modes !

A few examples ...

1. Nanowires with Rashba interaction

TOPOLOGICAL SUPERCONDUCTING NANOWIRE

Pairing of identical spin electrons is driven by the spin-orbit (Rashba) interaction in presence of the magnetic field, using semiconducting nanowires proximitized to the conventional (*s-wave*) superconductors.

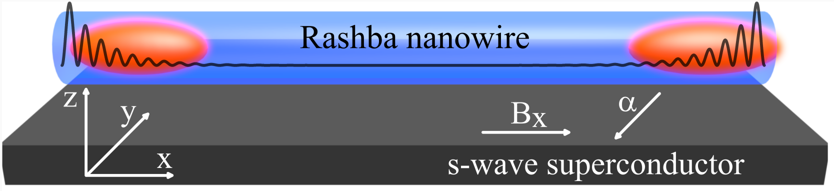

TOPOLOGICAL SUPERCONDUCTING NANOWIRE

Pairing of identical spin electrons is driven by the spin-orbit (Rashba) interaction in presence of the magnetic field, using semiconducting nanowires proximitized to the conventional (*s-wave*) superconductors.

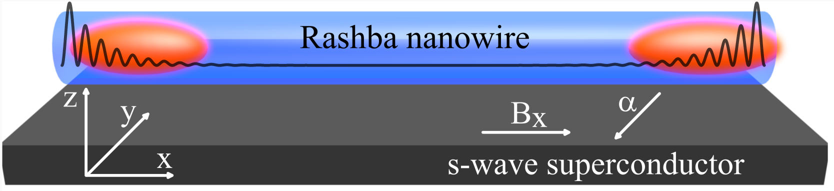

Examples: **nanowire = InSb, InAs, ...** **superconductor = Al, Pb, ...**

Effective quasiparticle states of the Rashba nanowire

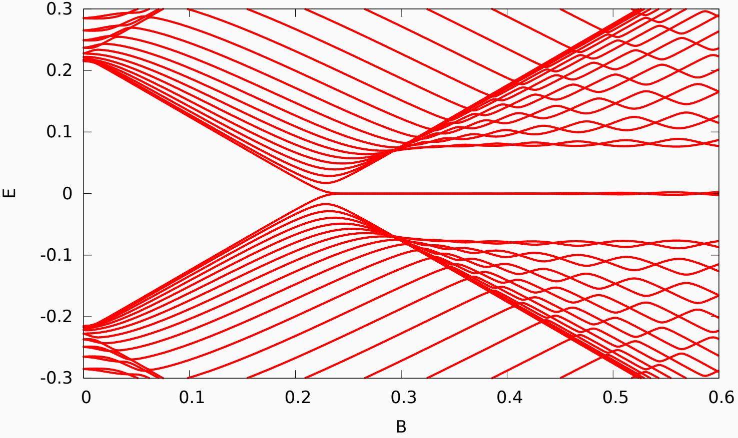

TRANSITION TO TOPOLOGICAL PHASE

Effective quasiparticle states of the Rashba nanowire

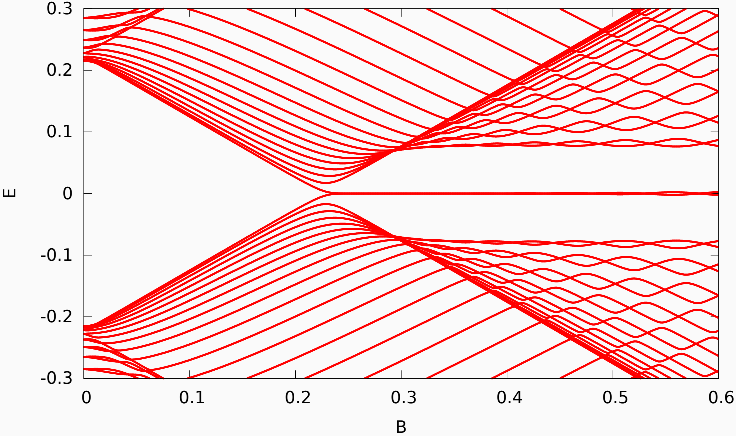

Closing/reopening of a gap ⇔ band-invertion of topological insulators

M.M. Maśka, A. Gorczyca-Goraj, J. Tworzydło, T. Domański, PRB 95, 045429 (2017).

Where do such Majoranas appear ?

Majorana qps are localized near the edges

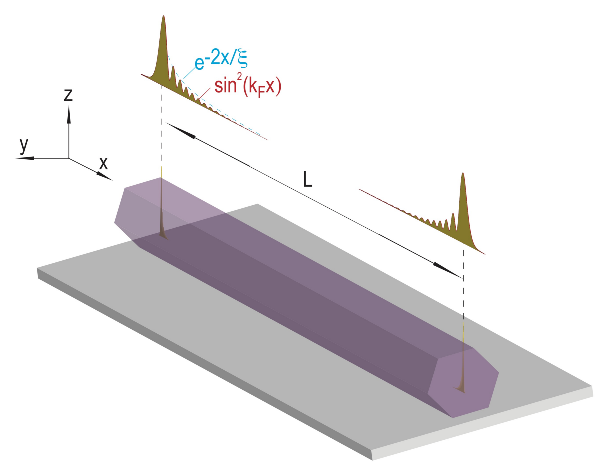

R. Aguado, Riv. Nuovo Cim. 40, 523 (2017).

Differential conductance dI/dV obtained for InSb nanowire at 70 mK upon varying a magnetic field.

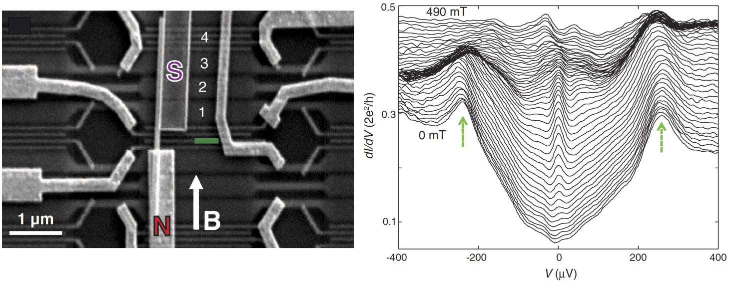

V. Mourik, ..., and L.P. Kouwenhoven, Science **336**, 1003 (2012).

/ Technical Univ. Delft, Netherlands /

Litographically fabricated Al nanowire contacted to InAs

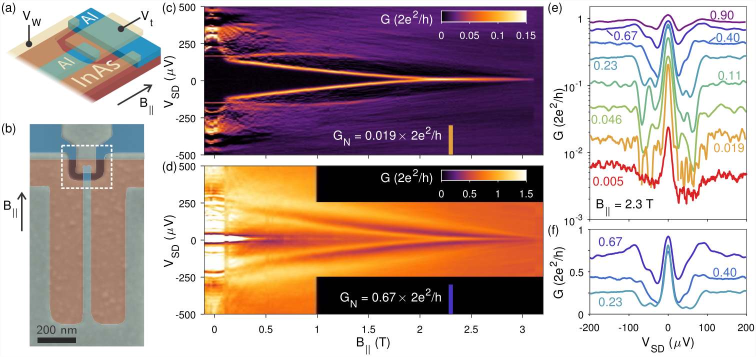

F. Nichele, ..., and Ch. Marcus, Phys. Rev. Lett. **119**, 136803 (2017).

/ Niels Bohr Institute, Copenhagen, Denmark /

Topological protection

Low energy quasiparticles of the Rashba nanowire

$t_{35}/t = 1.0$

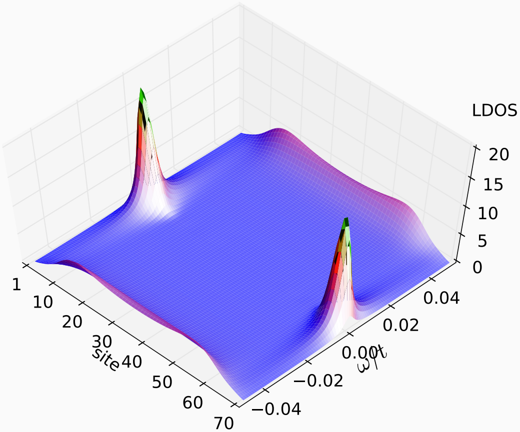

M.M. Maśka, A. Gorczyca-Goraj, J. Tworzydło, T. Domański, PRB 95, 045429 (2017).

Low energy quasiparticles of the Rashba nanowire

$t_{35}/t = 0.8$

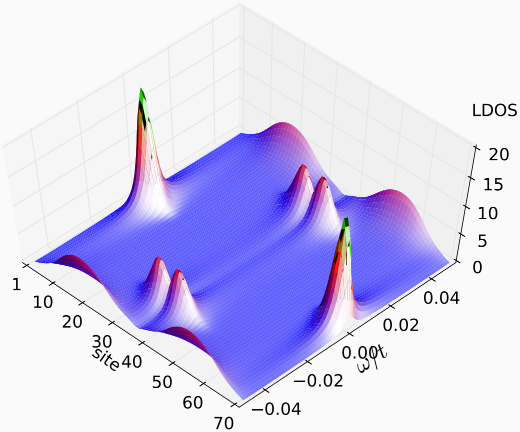

M.M. Maśka, A. Gorczyca-Goraj, J. Tworzydło, T. Domański, PRB 95, 045429 (2017).

Low energy quasiparticles of the Rashba nanowire

$t_{35}/t = 0.6$

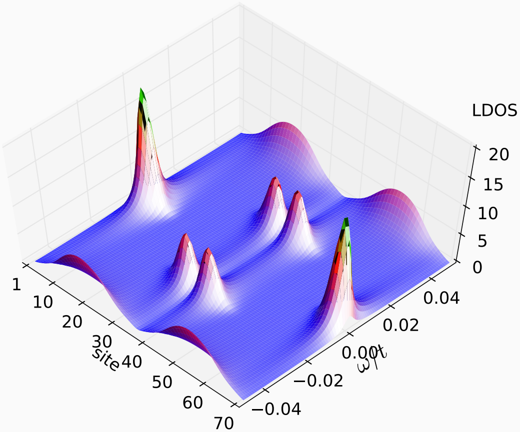

M.M. Maśka, A. Gorczyca-Goraj, J. Tworzydło, T. Domański, PRB 95, 045429 (2017).

Low energy quasiparticles of the Rashba nanowire

$t_{35}/t = 0.4$

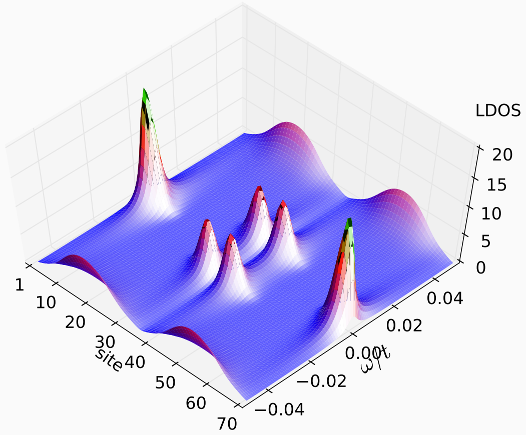

M.M. Maśka, A. Gorczyca-Goraj, J. Tworzydło, T. Domański, PRB 95, 045429 (2017).

Low energy quasiparticles of the Rashba nanowire

$t_{35}/t = 0.2$

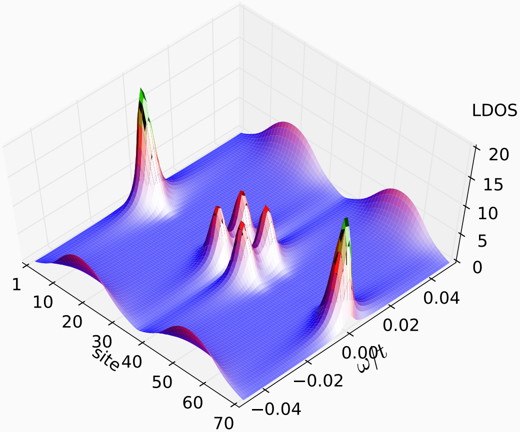

M.M. Maśka, A. Gorczyca-Goraj, J. Tworzydło, T. Domański, PRB 95, 045429 (2017).

Low energy quasiparticles of the Rashba nanowire

$t_{35}/t = 0.1$

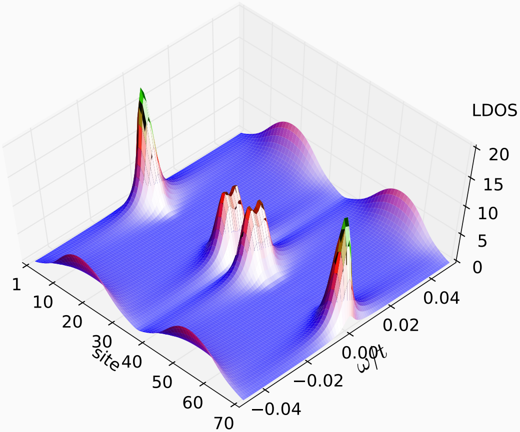

M.M. Maśka, A. Gorczyca-Goraj, J. Tworzydło, T. Domański, PRB 95, 045429 (2017).

Low energy quasiparticles of the Rashba nanowire

$t_{35}/t = 0.0$

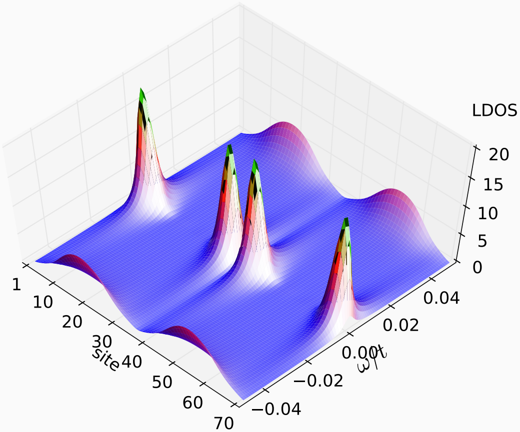

M.M. Maśka, A. Gorczyca-Goraj, J. Tworzydło, T. Domański, PRB 95, 045429 (2017).

2. Selforganized magnetic chains

MAGNETIC CHAINS ON SUPERCONDUCTORS

Magnetic atoms (like Fe) on a surface of s-wave superconductor (for example Pb) arrange themselves into such spiral order, where topological superconducting phase is selfsustained

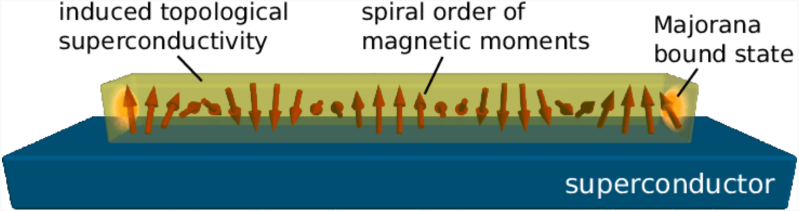

R. Lutchyn, J. Sau, S. Das Sarma, Phys. Rev. Lett. 105, 077001 (2010).

Y. Oreg, G. Refael, F. von Oppen, Phys. Rev. Lett. 105, 177002 (2010).

SPIRAL SELFORGANIZATION (TOPOFILIA)

A. Gorczyca-Goraj, T. Domański & M.M. Maśka, Phys. Rev. B 99, 235430 (2019).

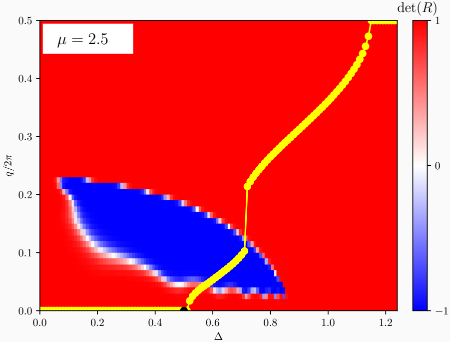

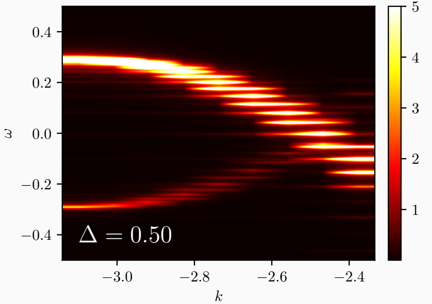

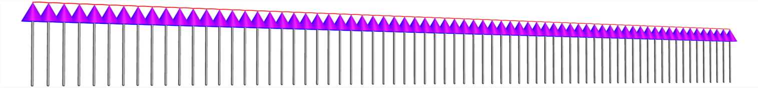

SPIRAL SELFORGANIZATION (TOPOFILIA)

A. Gorczyca-Goraj, T. Domański & M.M. Maśka, Phys. Rev. B 99, 235430 (2019).

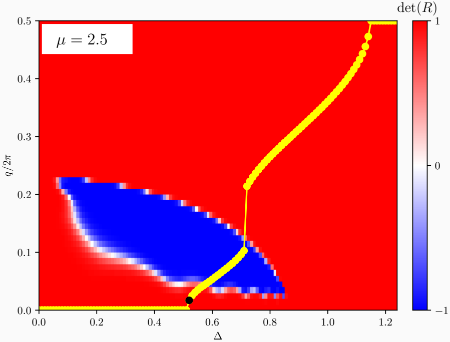

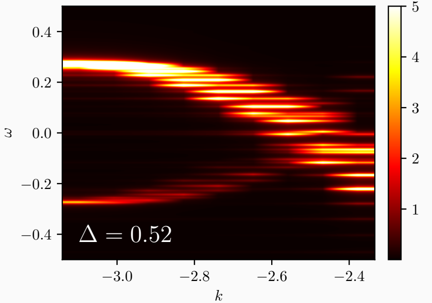

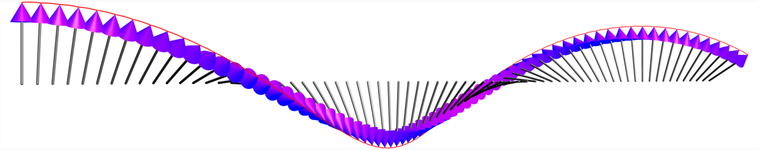

SPIRAL SELFORGANIZATION (TOPOFILIA)

A. Gorczyca-Goraj, T. Domański & M.M. Maśka, Phys. Rev. B <u>99</u>, 235430 (2019).

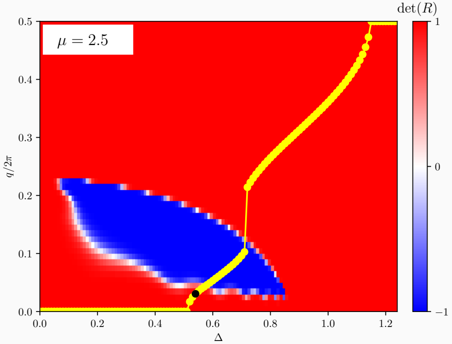

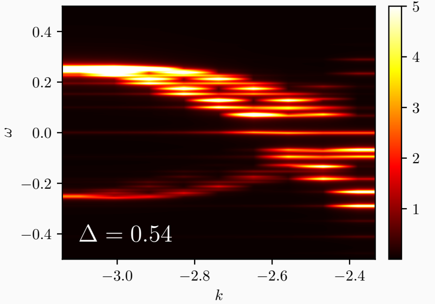

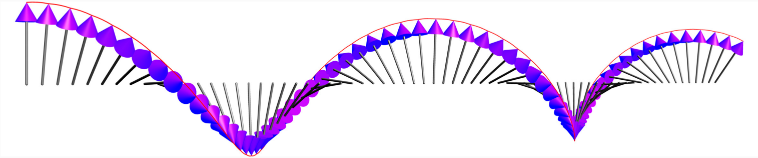

SPIRAL SELFORGANIZATION (TOPOFILIA)

A. Gorczyca-Goraj, T. Domański & M.M. Maśka, Phys. Rev. B 99, 235430 (2019).

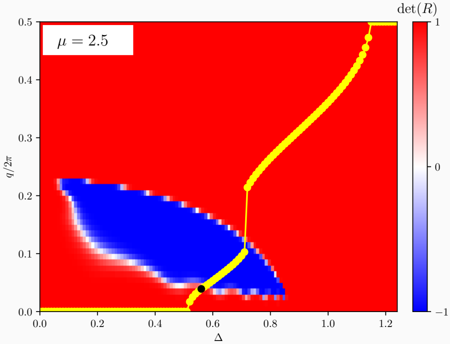

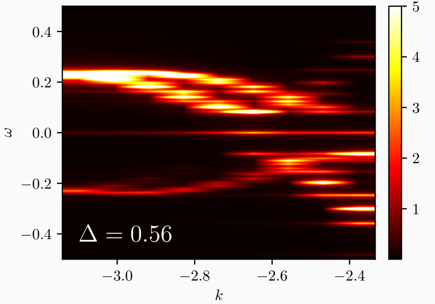

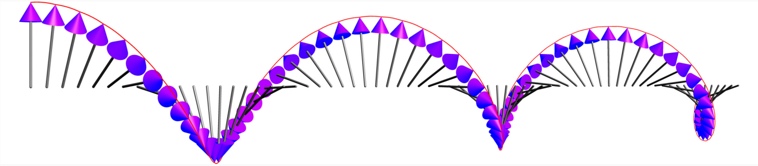

SPIRAL SELFORGANIZATION (TOPOFILIA)

A. Gorczyca-Goraj, T. Domański & M.M. Maśka, Phys. Rev. B <u>99</u>, 235430 (2019).

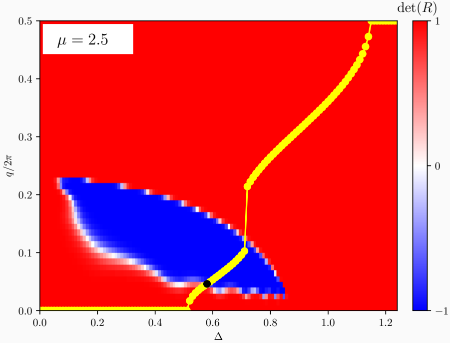

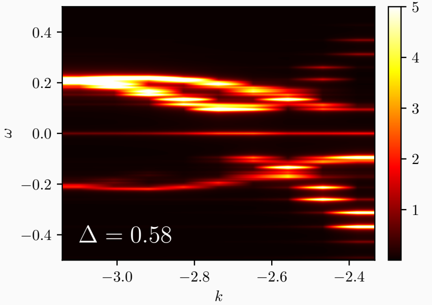

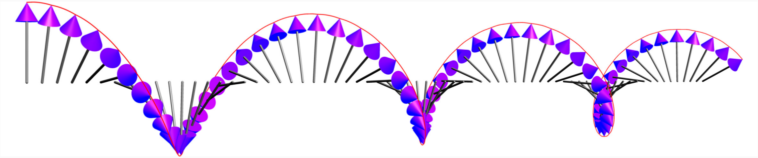

SPIRAL SELFORGANIZATION (TOPOFILIA)

A. Gorczyca-Goraj, T. Domański & M.M. Maśka, Phys. Rev. B 99, 235430 (2019).

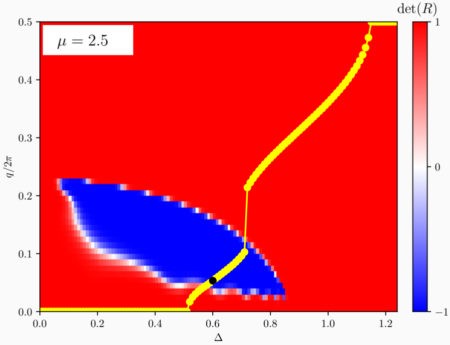

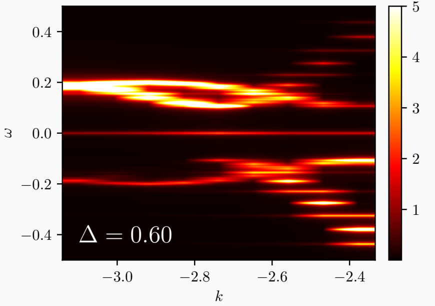

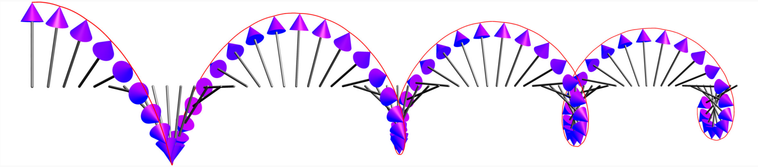

SPIRAL SELFORGANIZATION (TOPOFILIA)

A. Gorczyca-Goraj, T. Domański & M.M. Maśka, Phys. Rev. B 99, 235430 (2019).

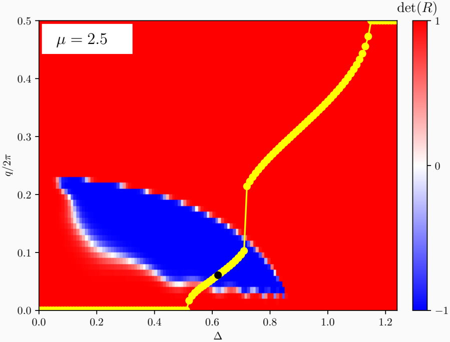

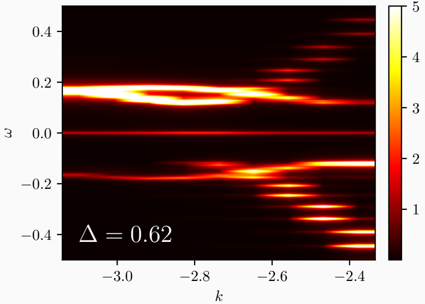

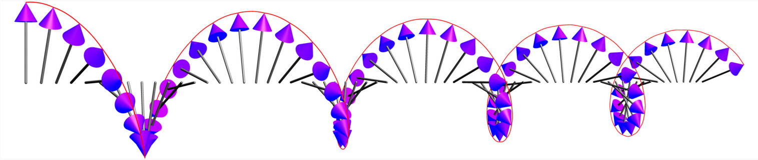

SPIRAL SELFORGANIZATION (TOPOFILIA)

A. Gorczyca-Goraj, T. Domański & M.M. Maśka, Phys. Rev. B 99, 235430 (2019).

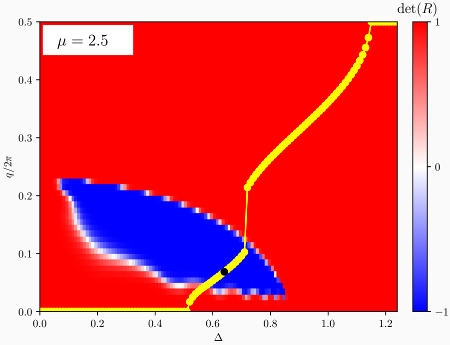

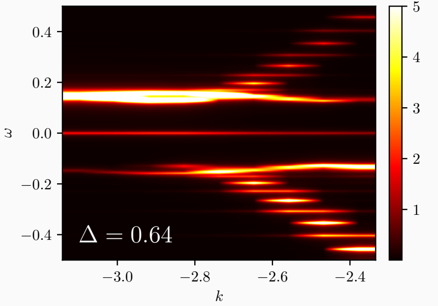

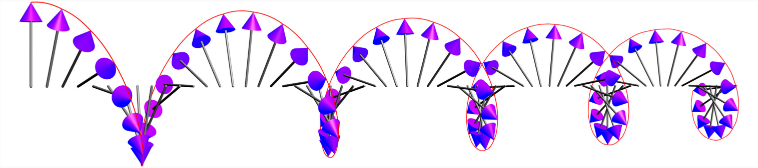

SPIRAL SELFORGANIZATION (TOPOFILIA)

A. Gorczyca-Goraj, T. Domański & M.M. Maśka, Phys. Rev. B <u>99</u>, 235430 (2019).

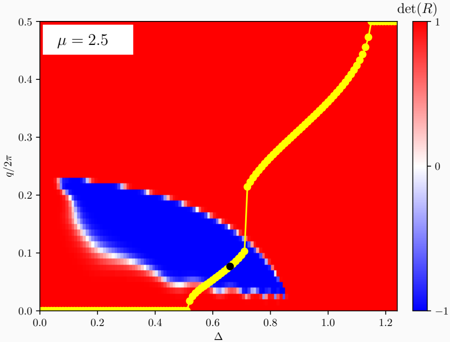

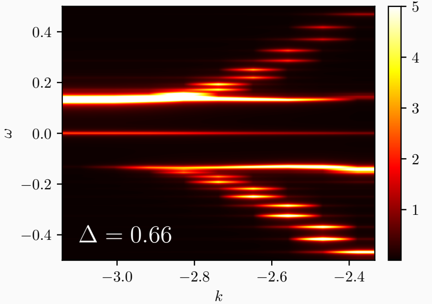

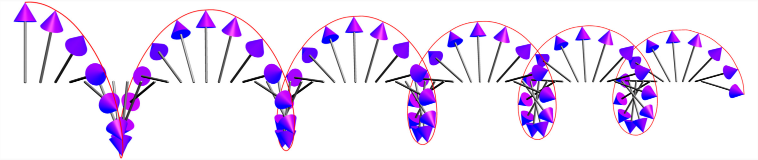

SPIRAL SELFORGANIZATION (TOPOFILIA)

A. Gorczyca-Goraj, T. Domański & M.M. Maśka, Phys. Rev. B 99, 235430 (2019).

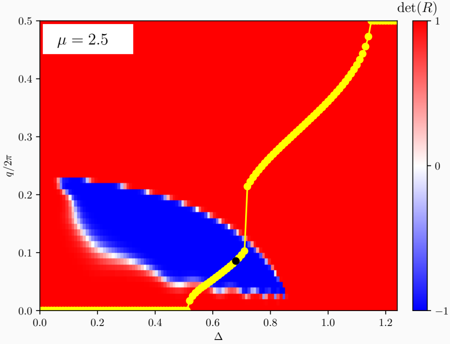

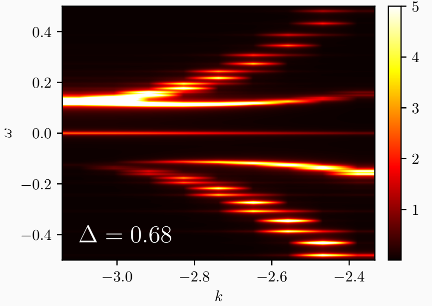

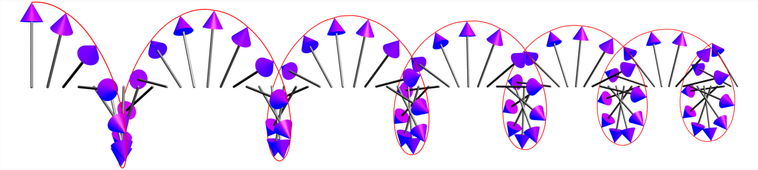

SPIRAL SELFORGANIZATION (TOPOFILIA)

A. Gorczyca-Goraj, T. Domański & M.M. Maśka, Phys. Rev. B 99, 235430 (2019).

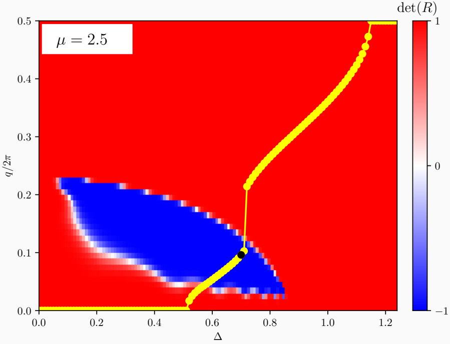

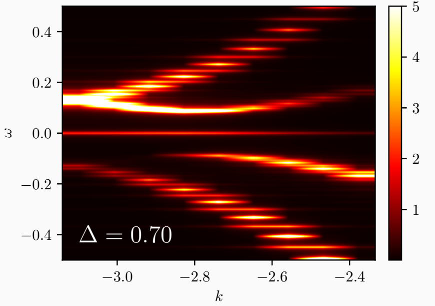

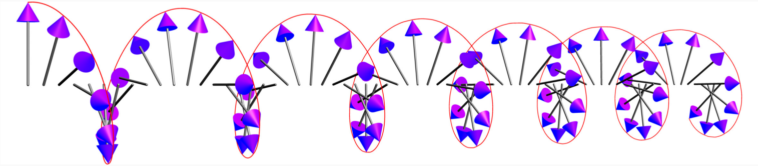

SPIRAL SELFORGANIZATION (TOPOFILIA)

A. Gorczyca-Goraj, T. Domański & M.M. Maśka, Phys. Rev. B 99, 235430 (2019).

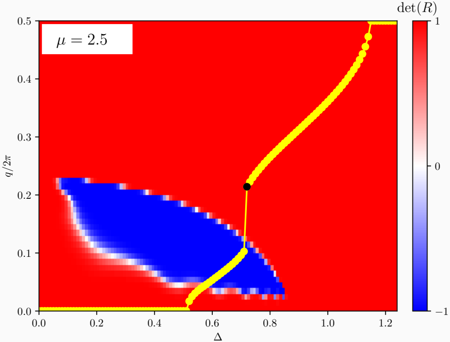

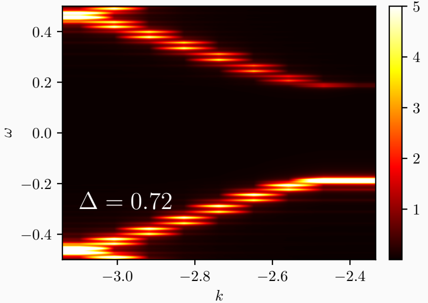

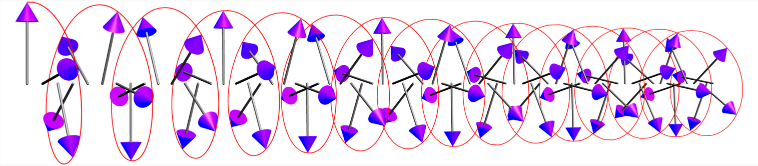

STM measurements for the nanochain of Fe atoms self-organized on a surface of superconducting Pb.

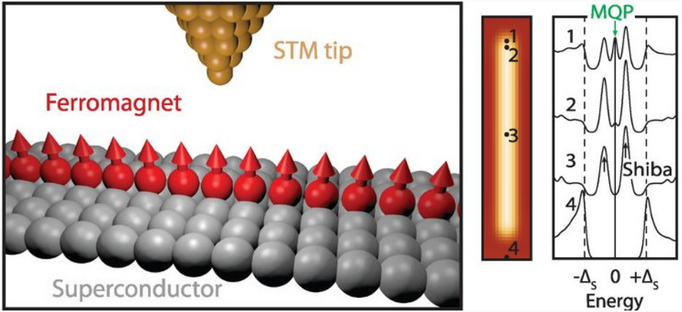

S. Nadj-Perge, ..., and A. Yazdani, Science **346**, 602 (2014).

/ Princeton University, USA /

AFM & STM data for Fe chain on Pb(110) surface

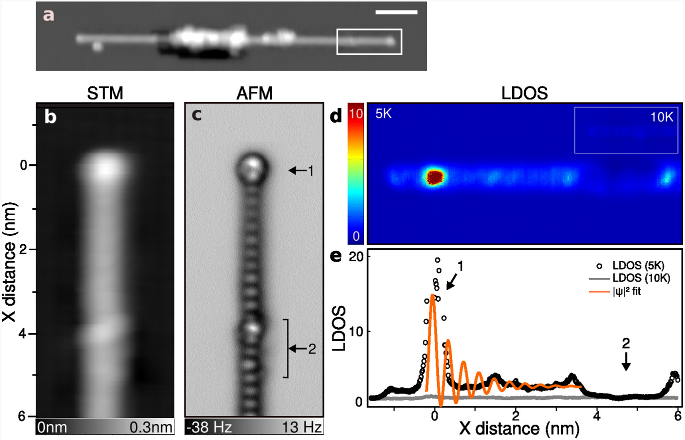

R. Pawlak, M. Kisiel *et al*, npj Quantum Information **2**, 16035 (2016).

/ University of Basel, Switzerland /

Majorana modes in Josephson junctions

PLANAR JOSEPHSON JUNCTIONS

Two-dimensional electron gas of InAs epitaxially covered by a thin Al layer

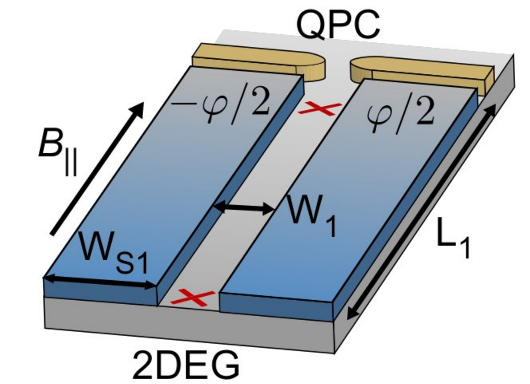

Width:

W_1 **= 80 nm**

Length:

L_1 **= 1.6** μ**m**

A. Fornieri, ..., Ch. Marcus and F. Nichele, Nature 569, 89 (2019).

Niels Bohr Institute (Copenhagen, Denmark)

Two-dimensional HgTe quantum well coupled to 15 nm thick Al film

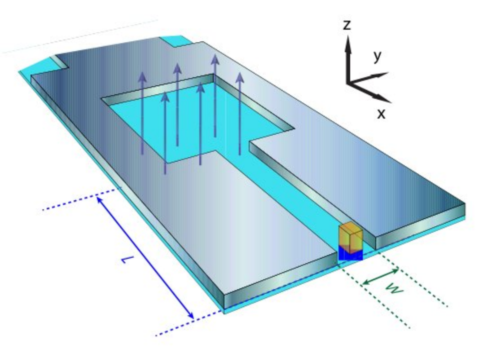

Width:

W = **600 nm**

Length:

L = **1.0 μm**

H. Ren, ..., L.W. Molenkamp, B.I. Halperin & A. Yacoby, Nature 569, 93 (2019).

Würzburg Univ. (Germany) + Harvard Univ. (USA)

TOPOGRAPHY OF MAJORANA MODES

Spatial profile of the zero-energy ($E_n = 0$) Majorana quasiparticles in a homogeneous metallic strip embedded into Josephson junction.

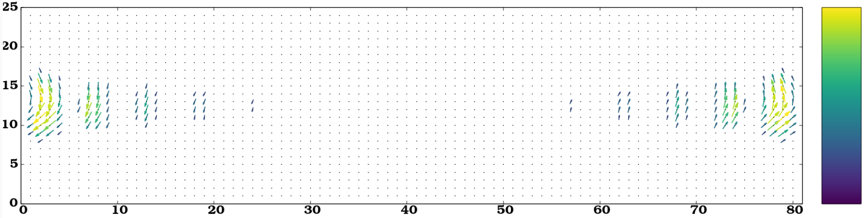

Sz. Głodzik, N. Sedlmayr & T. Domański, PRB 102, 085411 (2020).

LOCAL DEFECT IN JOSEPHSON JUNCTION

Spatial profile of the Majorana modes in presence of the strong electrostatic defect placed in the center.

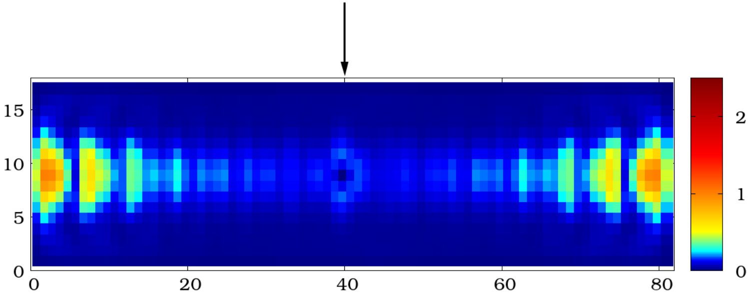

Sz. Głodzik, N. Sedlmayr & T. Domański, PRB 102, 085411 (2020).

LOCAL DEFECT IN JOSEPHSON JUNCTION

Spatial profile of the Majorana modes in presence of the strong electrostatic defect placed near the edge.

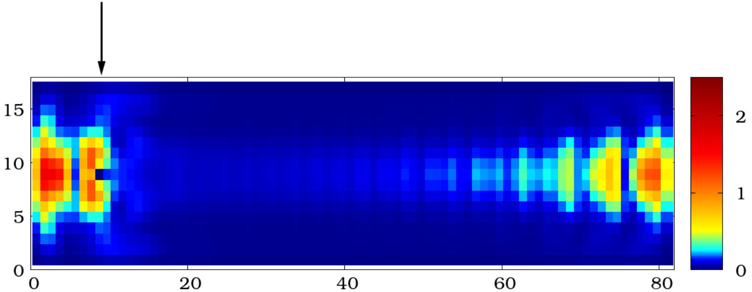

Sz. Głodzik, N. Sedlmayr & T. Domański, PRB 102, 085411 (2020).

Spatial profile of the Majorana modes in presence of the strong electrostatic defect placed near the edge.

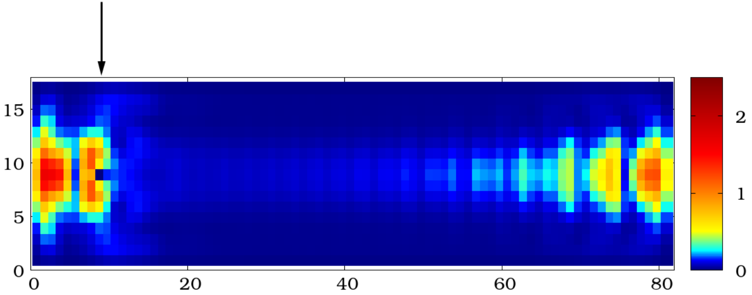

Sz. Głodzik, N. Sedlmayr & T. Domański, PRB 102, 085411 (2020).

"Benefits of Weak Disorder in One-Dimensional Topological Superconductors"
A. Haim & A. Stern, Phys. Rev. Lett. 122, 126801 (2019).

Higher-dimensional topological textures

Higher-dimensional topological textures

(platform for chiral Majorana modes)

Magnetic island of Co atoms deposited on the superconducting Pb surface

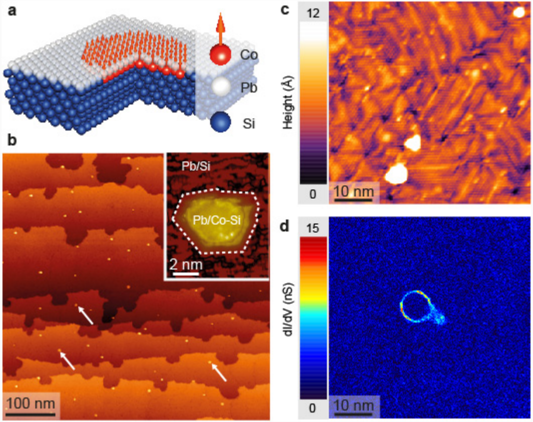

Diameter of island:

5 – 10 nm

G. Ménard, ..., and P. Simon, Nature Commun. 8, 2040 (2017).

Pierre & Marie Curie University (Paris, France)

Magnetic island of Fe atoms deposited on the superconducting Re surface

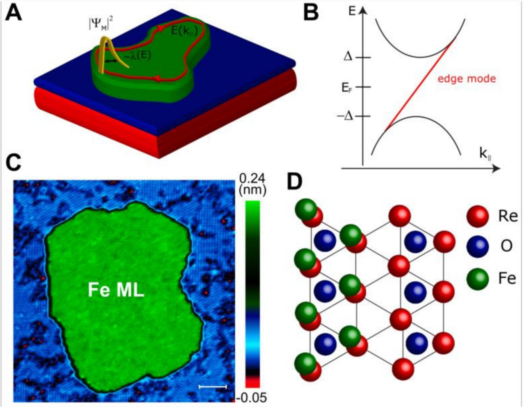

Chern number

C = 20

A. Palacio-Morales, ... & R. Wiesendanger, Science Adv. 5, eaav6600 (2019).

University of Hamburg (Germany)

VAN DER WAALS HETEROSTRUCTURES

Ferromagnetic island $CrBr_3$ deposited on superconducting $NbSe_2$

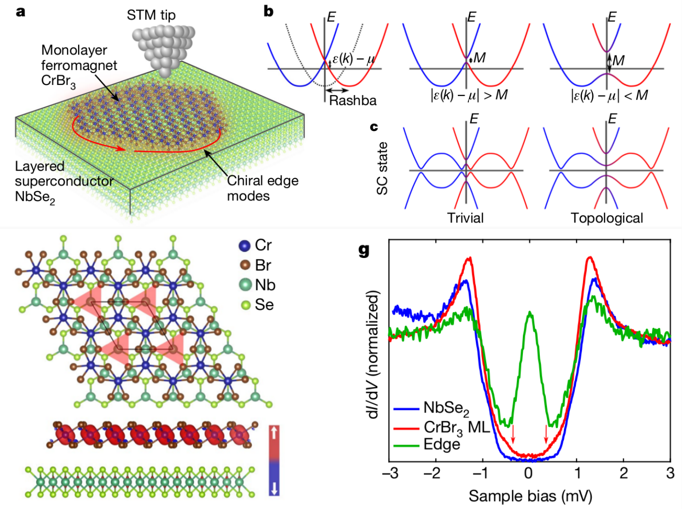

S. Kezilebieke ... Sz. Głodzik ... P. Lilieroth, Nature 424, 588 (2020).

Scenario for topological superconductivity induced in 2D magnetic thin film hosting a skyrmion deposited on conventional s-wave superconductor

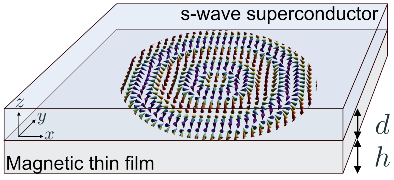

MAGNETIC SKYRMION-TYPE TEXTURES

Scenario for topological superconductivity induced in 2D magnetic thin film hosting a skyrmion deposited on conventional s-wave superconductor

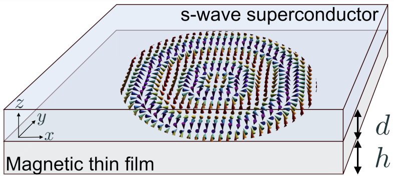

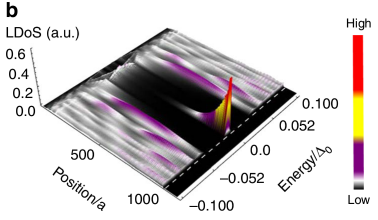

M. Garnier, A. Mesaros, P. Simon, Comm. Phys. 2, 126 (2019).

TAKE - HOME - MESSAGE

Synergy of semiconductor physics with electron pairing of superconductors in finite-size (dim=1 and dim=2) systems:

TAKE - HOME - MESSAGE

Synergy of semiconductor physics with electron pairing of superconductors in finite-size (dim=1 and dim=2) systems:

$\Rightarrow$ **can have constructive character,**

TAKE - HOME - MESSAGE

Synergy of semiconductor physics with electron pairing of superconductors in finite-size (dim=1 and dim=2) systems:

$\Longrightarrow$ **can have constructive character,**

$\Longrightarrow$ **leading to novel states of matter,**

TAKE - HOME - MESSAGE

Synergy of semiconductor physics with electron pairing of superconductors in finite-size (dim=1 and dim=2) systems:

$\Longrightarrow$ **can have constructive character,**

$\Longrightarrow$ **leading to novel states of matter,**

$\Longrightarrow$ **hosting the Majorana boundary modes,**

TAKE - HOME - MESSAGE

Synergy of semiconductor physics with electron pairing of superconductors in finite-size (dim=1 and dim=2) systems:

$\Rightarrow$ **can have constructive character,**

$\Rightarrow$ **leading to novel states of matter,**

$\Rightarrow$ **hosting the Majorana boundary modes,**

$\Rightarrow$ **useful for stable qubits & quantum computing.**

ACKNOWLEDGEMENTS

⇒ **Maciek Maśka**

(Technical University, Wrocław)

⇒ **Nick Sedlmayr**

(M. Curie-Skłodowska University, Lublin)

⇒ **Aksel Kobiałka**

(postdoc at University of Basel, Switzerland)

⇒ **Szczepan Głodzik**

(postdoc at University of Ljubljana, Slovenia)

TOPOLOGICAL INVARIANTS

Different homotopy groups:

TOPOLOGICAL INVARIANTS

Different homotopy groups:

dim=1 $\Rightarrow$ **homotopy group Z_2**

featured by the Berry phase ± 1 around the Brillouin zone

TOPOLOGICAL INVARIANTS

Different homotopy groups:

dim=1 $\Longrightarrow$ **homotopy group Z_2**

featured by the Berry phase ± 1 around the Brillouin zone

dim=2 $\Longrightarrow$ **homotopy group Z**

which can be characterized by the Chern number, that is equivalent to the Thouless–Kohmoto–Nightingale–den Nijs number.

TOPOLOGICAL INVARIANTS

Different homotopy groups:

dim=1 $\Rightarrow$ **homotopy group Z_2**

featured by the Berry phase ± 1 around the Brillouin zone

dim=2 $\Rightarrow$ **homotopy group Z**

which can be characterized by the Chern number, that is equivalent to the Thouless–Kohmoto–Nightingale–den Nijs number.

For details, concerning the topological criteria see e.g.

- **A. Kitaev, AIP Conf. Proc. 1134, 22 (2009);**
- **M.Z. Hasan & C.L. Kane, Rev. Mod. Phys. 82, 3045 (2010);**
- **X.-L. Qi & S.-C. Zhang, Rev. Mod. Phys. 83, 1057 (2011).**